Supporting Information: Pressure- and Aggregation-Induced Modulation of Linear and Nonlinear Optical Properties in a Push–Pull Chromophore: Insights from Computational Modelling

Josianne Owona,[†,‡,¶] Selom J. Goto,[†] Lionel Truflandier,[†] Claire Tonnelé,[*,¶,§] and Frédéric Castet[*,†]

†*Univ. Bordeaux, CNRS, Bordeaux INP, Institut des Sciences Moléculaires, UMR 5255, F-33400 Talence, France*

‡*Euskal Herriko Unibertsitatea, PK 1072, 20080 Donostia, Euskadi, Spain*

¶*Donostia International Physics Center, 20018 Donostia, Euskadi, Spain*

§*IKERBASQUE - Basque Foundation for Science, 48009 Bilbo, Euskadi, Spain*

E-mail: claire.tonnele@dipc.org; frederic.castet@u-bordeaux.fr

Contents

1 Electronic and Optical Properties of the Molecule

Table S1: Relative Gibbs free energies (ΔG, kcal/mol), room-temperature Maxwell-Boltzmann populations (P, %), dihedral angles (θ_1 and θ_2, degrees), Bond Length Alternation (BLA, Å) calculated along the the conjugated path illustrated in Figure S1), ground-state dipole moments (μ, D) and HOMO and LUMO energies (E_H and E_L, in eV), calculated at the CAM-B3LYP-D3/6-311G(d) level of theory for the four conformers of DPA-Th-DCV (represented in the Figure below).

Conformer	ΔG	P	θ_1	θ_2	BLA	μ	E_H	E_L
1	0.02	33.7	-1.2	29.7	0.026	10.48	-6.94	-1.74
2	0.48	15.5	178.3	30.7	0.027	11.67	-9.99	-1.80
3	0.45	16.1	178.5	30.9	0.027	11.69	-6.99	-1.80
4	0.00	34.7	-1.4	29.4	0.026	11.01	-6.94	-1.74

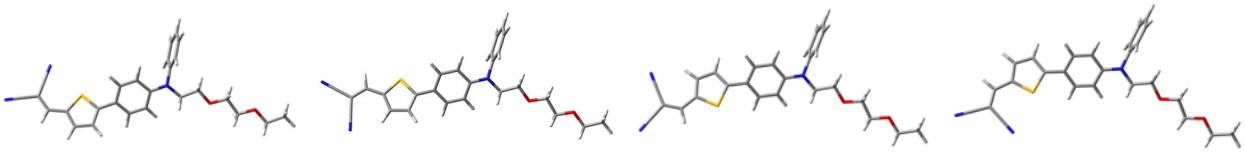

Conformer 1 Conformer 2 Conformer 3 Conformer 4

(a)

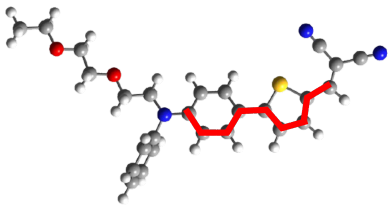

(b)

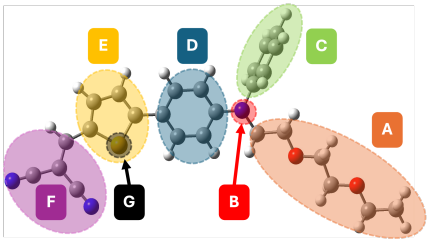

(c)

Units	Mulliken	NPA
A	+0.18	+0.33
B	-0.43	-0.49
C	+0.15	+0.21
D	+0.30	+0.13
E	+0.02	+0.12
F	-0.22	-0.20
G	+0.37	+0.44

Figure S1: (a) Optimized structure of the most stable conformer (conformer 4, see Table S1), with the conjugated path (highlighted in red) along which the bond length alternation path is calculated; (b) Fragments and their associated Mulliken and NPA charges (c) of conformer 4 in the ground state geometry, computed at the CAM-B3LYP-D3/6-311G(d) level of theory.

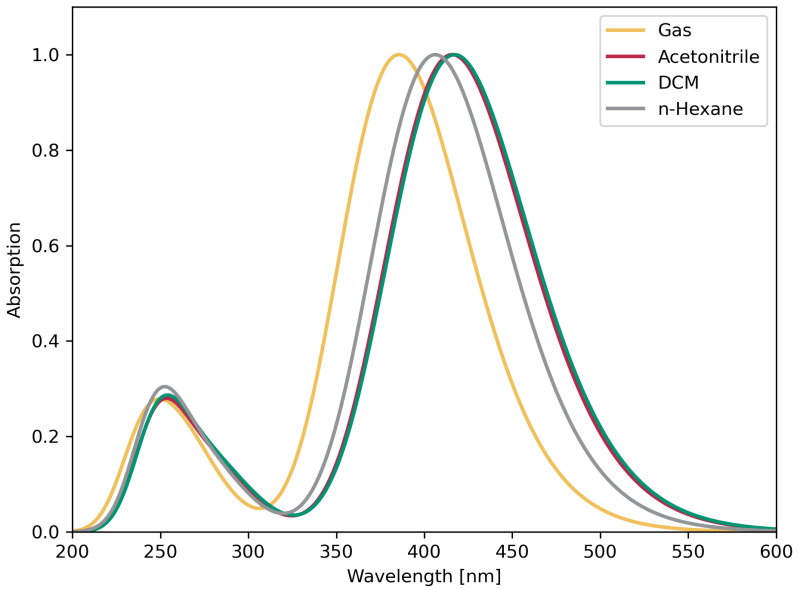

Figure S2: Absorption spectra of the molecule, calculated at the TDDFT/CAM-B3LYP-D3/6-311G(d) level in the gas phase and different solvents. The spectra were obtained by weighting the spectra of each conformer by their Maxwell-Boltzmann populations at room temperature (Table S1).

Table S2: Vertical excitation energies (ΔE, eV), wavelengths (λ, nm), oscillator strengths (f, dimensionless), electronic excitations and associated weights of the four conformers of DPA-Th-DCV, calculated at the TDDFT/CAM-B3LYP-D3/6-311G(d) in the **gas phase**. Only excited states with $f > 0.1$ are reported.

	State	ΔE (eV)	λ (nm)	f	Electronic transition	Weight
Conformer 1	1	3.25	381	1.07	HOMO-1 → LUMO	5%
					HOMO → LUMO	91%
	6	5.13	242	0.20	HOMO-6 → LUMO	3%
					HOMO → LUMO+1	42%
					HOMO → LUMO+3	42%
Conformer 2	1	3.25	381	1.22	HOMO-1 → LUMO	6%
					HOMO → LUMO	90%
	6	5.05	246	0.16	HOMO-6 → LUMO	2%
					HOMO-1 → LUMO+3	2%
					HOMO → LUMO+1	38%
					HOMO → LUMO+3	44%
Conformer 3	1	3.25	381	1.22	HOMO-1 → LUMO	6%
					HOMO → LUMO	90%
	6	5.06	245	0.15	HOMO-1 → LUMO+3	2%
					HOMO → LUMO+1	34%
					HOMO → LUMO+3	49%
Conformer 4	1	3.25	381	1.11	HOMO-1 → LUMO	5%
					HOMO → LUMO	91%
	4	4.73	262	0.10	HOMO-6 → LUMO	53%
					HOMO-5 → LUMO	10%
					HOMO-2 → LUMO	2%
	6	5.12	242	0.16	HOMO-1 → LUMO	27%
					HOMO-2 → LUMO	3%
					HOMO-1 → LUMO+2	3%
					HOMO → LUMO+1	40%
					HOMO → LUMO+3	40%

Table S3: Vertical excitation energies (ΔE, eV), wavelengths (λ, nm), oscillator strengths (f, dimensionless), electronic excitations and associated weights of the four conformers of DPA-Th-DCV, calculated at the TDDFT/CAM-B3LYP-D3/6-311G(d) in **dichloromethane**. Only excited states with $f > 0.1$ are reported.

	State	ΔE (eV)	λ (nm)	f	Electronic transition	Weight
Conformer 1	1	2.98	416	1.08	HOMO-1 → LUMO	5%
					HOMO → LUMO	92%
	5	4.95	250	0.14	HOMO-5 → LUMO	5%
					HOMO-4 → LUMO	11%
					HOMO-2 → LUMO	3%
					HOMO → LUMO+1	55%
					HOMO → LUMO+2	12%
					HOMO → LUMO+4	2%
Conformer 2	1	2.96	419	1.19	HOMO-1 → LUMO	5%
					HOMO → LUMO	91%
	5	4.86	255	0.22	HOMO → LUMO+1	86%
Conformer 3	1	2.96	419	1.20	HOMO-1 → LUMO	5%
					HOMO → LUMO	91%
	2	4.28	290	0.11	HOMO-8 → LUMO	2%
					HOMO-7 → LUMO	4%
					HOMO-1 → LUMO	85%
					HOMO → LUMO	4%
	5	4.86	255	0.22	HOMO → LUMO+1	86%
Conformer 4	1	2.98	416	1.11	HOMO-1 → LUMO	5%
					HOMO → LUMO	92%
	5	4.96	250	0.19	HOMO-4 → LUMO	2%
					HOMO → LUMO+1	75%
					HOMO → LUMO+4	7%

Table S4: Vertical excitation energies (ΔE, eV), wavelengths (λ, nm), oscillator strengths (f, dimensionless), electronic excitations and associated weights the four conformers of DPA-Th-DCV, calculated at the TDDFT/CAM-B3LYP-D3/6-311G(d) in **acetonitrile**. Only excited states with $f > 0.1$ are reported.

	State	ΔE (eV)	λ (nm)	f	Electronic transition	Weight
Conformer 1	1	2.99	415	1.09	HOMO-1 → LUMO	5%
					HOMO → LUMO	92%
	5	4.97	250	0.15	HOMO-5 → LUMO	4%
					HOMO-4 → LUMO	8%
					HOMO-2 → LUMO	2%
					HOMO → LUMO+1	62%
					HOMO → LUMO+2	8%
					HOMO → LUMO+4	3%
	6	5.00	248	0.12	HOMO-7 → LUMO	6%
					HOMO-5 → LUMO	10%
					HOMO-4 → LUMO	19%
					114 → LUMO	4%
					HOMO-2 → LUMO	6%
					HOMO → LUMO+1	19%
					HOMO → LUMO+2	26%
					HOMO → LUMO+4	3%
Conformer 2	1	2.97	418	1.21	HOMO-1 → LUMO	5%
					HOMO → LUMO	91%
	5	4.86	255	0.22	HOMO → LUMO+1	86%
Conformer 3	1	2.97	418	1.21	HOMO-1 → LUMO	5%
					HOMO → LUMO	91%
	2	4.29	289	0.10	HOMO-7 → LUMO	5%
					HOMO-1 → LUMO	85%
					HOMO → LUMO	4%
	5	4.87	255	0.22	HOMO → LUMO+1	86%
Conformer 4	1	2.99	415	1.12	HOMO-1 → LUMO	5%
					HOMO → LUMO	92%
	5	4.97	250	0.19	HOMO → LUMO+1	78%
					HOMO → LUMO+4	7%

Table S5: Vertical excitation energies (ΔE, eV), wavelengths (λ, nm), oscillator strengths (f, dimensionless), electronic excitations and associated weights of the four conformers of DPA-Th-DCV, calculated at the TDDFT/CAM-B3LYP-D3/6-311G(d) in **hexane**. Only excited states with $f > 0.1$ are reported.

	State	ΔE (eV)	λ (nm)	f	Electronic transition	Weight
Conformer 1	1	3.06	406	1.06	HOMO-1 → LUMO	5%
					HOMO → LUMO	91%
	5	4.97	250	0.18	HOMO-4 → LUMO	2%
					HOMO-1 → LUMO+3	3%
					HOMO → LUMO+1	68%
					HOMO → LUMO+2	2%
					HOMO → LUMO+3	13%
Conformer 2	1	3.04	407	1.18	HOMO-1 → LUMO	6%
					HOMO → LUMO	91%
	5	4.89	254	0.24	HOMO → LUMO+1	82%
					HOMO → LUMO+3	4%
Conformer 3	1	3.04	407	1.18	HOMO-1 → LUMO	6%
					HOMO → LUMO	90%
	5	4.88	254	0.22	HOMO-7 → LUMO	2%
					HOMO → LUMO+1	81%
					HOMO → LUMO+3	5%
Conformer 4	1	3.06	406	1.09	HOMO-1 → LUMO	5%
					HOMO → LUMO	91%
	5	4.96	250	0.15	HOMO-1 → LUMO+3	4%
					HOMO → LUMO+1	64%
					HOMO → LUMO+3	20%

Table S6: Characteristics of the charge transfer (CT) parameters related to the $S_0 \rightarrow S_1$ transition in conformer 1-4, calculated at the CAM-B3LYP-D3/6-311G(d) in acetonitrile, dichloromethane, and hexane: amount of charge transferred (ρ, $|e|$), charge transfer distance (Å) and dipole moment variation ($\Delta\mu$, D).

	Conformer 1	Conformer 2	Conformer 3	Conformer 4
			Acetonitrile	
ρ (eV)	0.647	0.650	0.650	0.647
CT distance (Å)	3.202	3.435	3.476	3.217
$\Delta\mu$(D)	9.944	10.729	10.859	10.003
			Dichloromethane	
ρ (eV)	0.652	0.659	0.658	0.653
CT distance (Å)	3.225	3.462	3.500	3.243
$\Delta\mu$ (D)	10.098	10.953	11.065	10.179
			Hexane	
ρ (eV)	0.660	0.664	0.665	0.658
CT distance (Å)	3.243	3.483	3.492	3.268
$\Delta\mu$ (D)	10.276	11.109	11.154	10.325

Table S7: Static and dynamic components of first hyperpolarizability vector and anisotropy of the NLO response in conformers 1-4, calculated at the CAM-B3LYP-D3/6-311G(d) in the gas phase. The Cartesian frame used for the NLO calculations, corresponding to the Gaussian standard orientation (in which Cartesian axes are aligned along the principal moments of inertia), is shown in the Figure above for the most stable conformer.

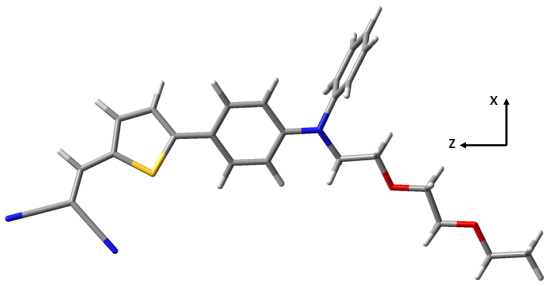

	Static					Dynamic				
Conformer	$\lvert\beta_{zzz}\rvert$	$\lvert\beta_z\rvert$	$\lvert\beta_{xy}\rvert$	β	α_β	$\lvert\beta_{zzz}\rvert$	$\lvert\beta_z\rvert$	$\lvert\beta_{xy}\rvert$	β	α_β
1	12772	12687	1639	12792	7.7	226413	227092	18917	227879	12.0
2	13792	13699	1721	13807	8.0	259283	263688	38685	266511	6.8
3	12883	13472	3707	13973	3.6	248435	262780	65884	270913	4.0
4	11838	12640	3729	13179	3.4	201802	225982	79347	239508	2.8

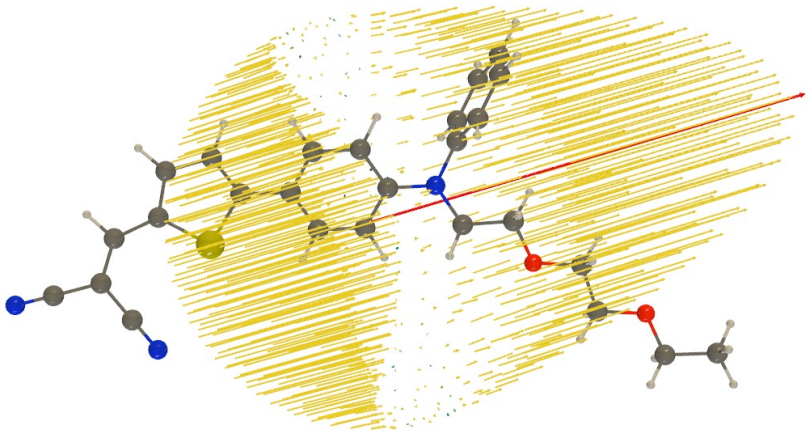

Figure S3: Unit sphere representation (yellow arrows) of the static first hyperpolarizability tensor of the molecule. The red arrow represents the first hyperpolarizability vector.

2 Crystal Structure Properties

Table S8: Comparison of the calculated and experimental lattice parameters, including translation vectors a, b, c (Å) and angles α, β, γ (degrees), of the crystal structure of compound 1. See Figure 1 of the main text for the definition of the crystal axes.

Parameter	Exp.	Calc.	Deviation (%)
a	6.89	6.66	-3.34
b	13.74	14.11	2.69
c	26.72	26.82	0.37
α	99.82	101.30	1.48
β	96.04	96.58	0.56
γ	95.03	95.92	0.94

Table S9: Lattice parameters, including translation vectors a, b, c (Å) and angles α, β, γ (degrees), computed under increasing isotropic pressures (kbar).

Pressure	a	b	c	α	β	γ
1	6.60	14.14	26.74	101.49	96.56	94.80
2	6.65	13.90	26.62	101.38	96.61	95.04
3	6.65	13.77	26.52	101.27	96.66	95.13
4	6.65	13.68	26.44	101.17	96.67	95.16
5	6.67	13.56	26.35	101.51	96.56	95.35
6	6.67	13.49	26.27	101.52	96.56	95.37
7	6.66	13.42	26.20	101.51	96.59	95.39
8	6.66	13.35	26.14	101.47	96.64	95.40
9	6.65	13.30	26.09	101.51	96.64	95.42
10	6.70	13.06	25.93	100.55	96.25	95.22
11	6.69	13.02	25.89	100.50	96.30	95.21
12	6.67	13.04	25.86	100.62	96.34	95.10
13	6.68	12.94	25.83	100.66	96.36	95.28
14	6.65	12.93	25.79	100.66	96.40	95.11
15	6.67	12.85	25.74	100.24	96.46	95.27
16	6.64	12.87	25.74	100.43	96.47	95.14
17	6.66	12.77	25.67	100.13	96.55	95.29
18	6.63	12.79	25.67	100.26	96.56	95.12
19	6.63	12.75	25.63	100.15	96.62	95.13
20	6.62	12.72	25.59	99.98	96.67	95.15
21	6.62	12.68	25.57	99.99	96.69	95.14
22	6.62	12.64	25.54	99.85	96.74	95.16
23	6.61	12.61	25.50	99.67	96.77	95.18
24	6.62	12.57	25.42	99.16	96.84	95.20
25	6.62	12.52	25.40	99.01	96.88	95.27
26	6.62	12.47	25.40	98.94	96.92	95.29
27	6.61	12.44	25.37	98.84	96.94	95.30
28	6.66	12.29	25.12	96.57	96.94	95.65
29	6.65	12.29	25.12	96.73	96.92	95.68
30	6.64	12.27	25.11	96.74	96.95	95.63

Table S10: Molecular parameters (torsional and stacking angles, in degrees) computed under increasing isotropic pressures.

	Torsional angles				Stacking angles	
Pressure	θ_1 (mon. 1)	θ_1 (mon. 2)	θ_2 (mon. 1)	θ_2 (mon. 2)	γ_1	γ_2
0	9.70	-0.54	3.97	-5.28	42.55	34.15
1	9.68	-0.37	3.80	-4.81	43.75	35.87
2	9.55	-0.64	3.53	-5.18	40.62	32.29
3	9.69	-0.67	3.22	-5.33	39.17	30.70
4	9.69	-0.72	2.83	-5.17	38.32	29.64
5	10.48	-0.97	2.33	-5.20	36.90	27.09
6	10.79	-1.05	1.92	-5.08	36.30	25.91
7	11.28	-1.27	1.45	-4.85	35.71	24.48
8	11.80	-1.43	0.97	-4.87	35.24	23.10
9	11.96	-1.52	0.73	-4.80	34.90	22.63
10	24.16	-6.23	-11.47	-0.24	24.50	7.53
11	24.03	-6.26	-11.54	-0.13	24.62	7.48
12	24.31	-6.07	-11.57	-0.03	24.59	7.71
13	23.76	-6.16	-11.69	-0.01	23.86	7.82
14	24.12	-6.35	-11.60	0.16	24.34	8.09
15	23.76	-7.01	-11.66	0.55	23.58	9.04
16	24.16	-7.07	-11.81	0.60	23.99	9.15
17	23.69	-7.46	-11.59	0.84	23.26	9.56
18	24.10	-7.55	-11.87	1.10	23.68	9.95
19	24.06	-7.87	-11.96	1.29	23.47	10.44
20	24.07	-8.27	-11.84	1.53	23.17	11.18
21	23.97	-8.28	-11.85	1.58	23.08	11.17
22	23.92	-8.68	-11.93	1.97	22.85	11.76
23	23.88	-9.04	-11.84	2.17	22.51	12.36
24	23.85	-10.18	-11.88	3.14	21.86	14.15
25	23.73	-10.39	-11.87	3.34	21.36	14.46
26	23.63	-10.37	-11.76	3.48	21.16	14.49
27	23.53	-10.84	-11.80	3.84	20.98	15.10
28	21.23	-15.68	-8.79	8.03	14.08	22.18
29	21.22	-15.05	-8.69	7.54	14.60	20.96
30	21.27	-14.85	-8.65	7.29	14.90	20.59

Table S11: Molecular parameters (bond lengths, in Å) computed under increasing isotropic pressures. Atom labels correspond to the Figure above the table.

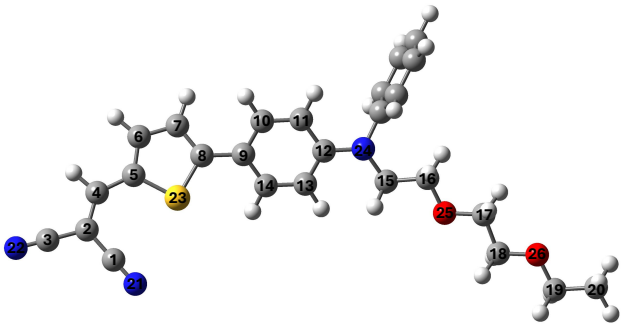

(a) **Monomer 1**

Pressure	C4-C5	C5-C6	C6-C7	C7-C8	C8-C9	C9-C10	C10-C11	C11-C12
0	1.40	1.40	1.39	1.40	1.44	1.41	1.38	1.42
1	1.40	1.40	1.39	1.40	1.44	1.42	1.38	1.42
2	1.40	1.41	1.39	1.40	1.44	1.41	1.38	1.42
3	1.40	1.40	1.39	1.40	1.44	1.41	1.38	1.42
4	1.40	1.40	1.39	1.40	1.44	1.41	1.38	1.42
5	1.40	1.40	1.39	1.40	1.44	1.41	1.38	1.42
6	1.40	1.40	1.39	1.40	1.44	1.41	1.38	1.42
7	1.40	1.40	1.39	1.40	1.44	1.41	1.38	1.42
8	1.40	1.40	1.39	1.40	1.44	1.41	1.38	1.42
9	1.40	1.40	1.39	1.40	1.44	1.41	1.38	1.42
10	1.40	1.40	1.39	1.40	1.44	1.41	1.38	1.42
11	1.40	1.40	1.39	1.40	1.44	1.41	1.38	1.42
12	1.40	1.41	1.39	1.40	1.44	1.40	1.38	1.42
13	1.40	1.40	1.39	1.40	1.44	1.41	1.38	1.42
14	1.40	1.40	1.39	1.40	1.44	1.40	1.38	1.42
15	1.40	1.40	1.39	1.40	1.44	1.40	1.38	1.42
16	1.40	1.40	1.39	1.40	1.44	1.40	1.38	1.42
17	1.40	1.40	1.39	1.40	1.44	1.40	1.38	1.42
18	1.40	1.40	1.39	1.40	1.44	1.40	1.38	1.42
19	1.40	1.40	1.39	1.40	1.44	1.40	1.38	1.42
20	1.40	1.40	1.39	1.40	1.44	1.40	1.38	1.42
21	1.40	1.40	1.39	1.40	1.44	1.40	1.38	1.42
22	1.40	1.40	1.39	1.40	1.44	1.40	1.37	1.42
23	1.40	1.40	1.39	1.40	1.44	1.40	1.38	1.42
24	1.40	1.40	1.39	1.40	1.44	1.40	1.38	1.42
25	1.40	1.40	1.39	1.40	1.44	1.40	1.38	1.42
26	1.40	1.40	1.39	1.40	1.43	1.40	1.37	1.42
27	1.40	1.40	1.39	1.40	1.44	1.40	1.37	1.42
28	1.40	1.40	1.39	1.40	1.43	1.40	1.37	1.42
29	1.40	1.40	1.39	1.40	1.43	1.40	1.37	1.42
30	1.40	1.40	1.39	1.40	1.44	1.40	1.37	1.42

(b) **Monomer 2**

Pressure	C4-C5	C5-C6	C6-C7	C7-C8	C8-C9	C9-C10	C10-C11	C11-C12
0	1.40	1.41	1.39	1.41	1.44	1.42	1.38	1.42
1	1.41	1.40	1.39	1.40	1.44	1.42	1.38	1.42
2	1.41	1.40	1.39	1.40	1.44	1.42	1.38	1.42
3	1.40	1.40	1.39	1.40	1.44	1.42	1.38	1.42
4	1.40	1.40	1.39	1.41	1.44	1.42	1.38	1.42
5	1.40	1.40	1.39	1.40	1.44	1.42	1.38	1.42
6	1.40	1.40	1.39	1.40	1.44	1.42	1.38	1.42
7	1.40	1.40	1.39	1.40	1.44	1.41	1.38	1.42
8	1.40	1.40	1.39	1.40	1.44	1.42	1.38	1.42
9	1.40	1.40	1.39	1.40	1.44	1.42	1.38	1.42
10	1.40	1.40	1.39	1.40	1.44	1.41	1.38	1.42
11	1.40	1.40	1.39	1.40	1.44	1.41	1.38	1.42
12	1.40	1.40	1.39	1.40	1.44	1.41	1.38	1.42
13	1.40	1.40	1.39	1.40	1.44	1.41	1.38	1.42
14	1.40	1.40	1.39	1.40	1.43	1.41	1.38	1.42
15	1.40	1.40	1.39	1.40	1.43	1.41	1.38	1.42
16	1.40	1.40	1.39	1.40	1.43	1.41	1.38	1.42
17	1.40	1.40	1.39	1.40	1.43	1.41	1.38	1.42
18	1.40	1.40	1.39	1.40	1.43	1.41	1.38	1.42
19	1.40	1.40	1.39	1.40	1.43	1.41	1.38	1.42
20	1.40	1.40	1.39	1.40	1.43	1.41	1.38	1.42
21	1.40	1.40	1.39	1.40	1.43	1.41	1.38	1.42
22	1.40	1.40	1.39	1.40	1.43	1.41	1.38	1.42
23	1.40	1.40	1.39	1.40	1.43	1.41	1.38	1.42
24	1.40	1.40	1.39	1.40	1.43	1.41	1.38	1.42
25	1.40	1.40	1.39	1.40	1.43	1.41	1.38	1.42
26	1.40	1.40	1.39	1.40	1.43	1.41	1.38	1.42
27	1.40	1.40	1.39	1.40	1.43	1.41	1.38	1.42
28	1.40	1.41	1.39	1.40	1.43	1.41	1.37	1.42
29	1.40	1.41	1.39	1.40	1.43	1.41	1.37	1.42
30	1.39	1.41	1.39	1.40	1.43	1.41	1.37	1.42

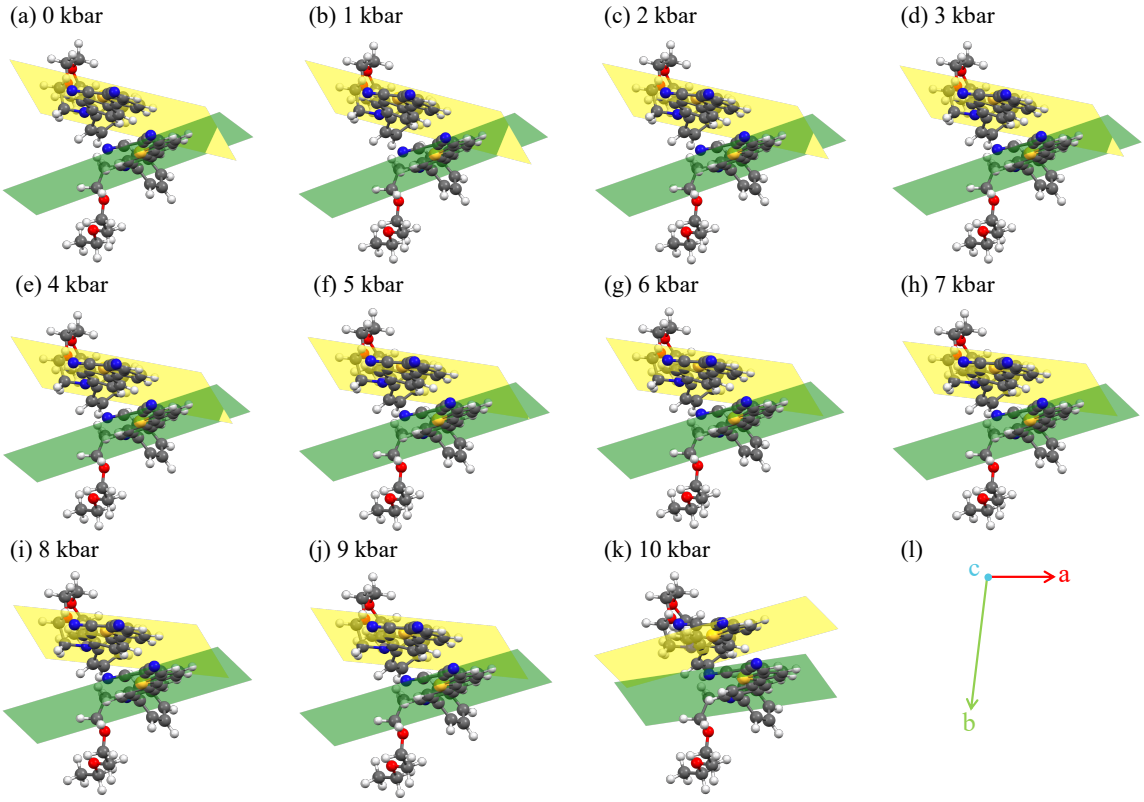

Figure S4: Evolution with pressure of the stacking angle between the planes of the thiophenyl rings (γ_2).

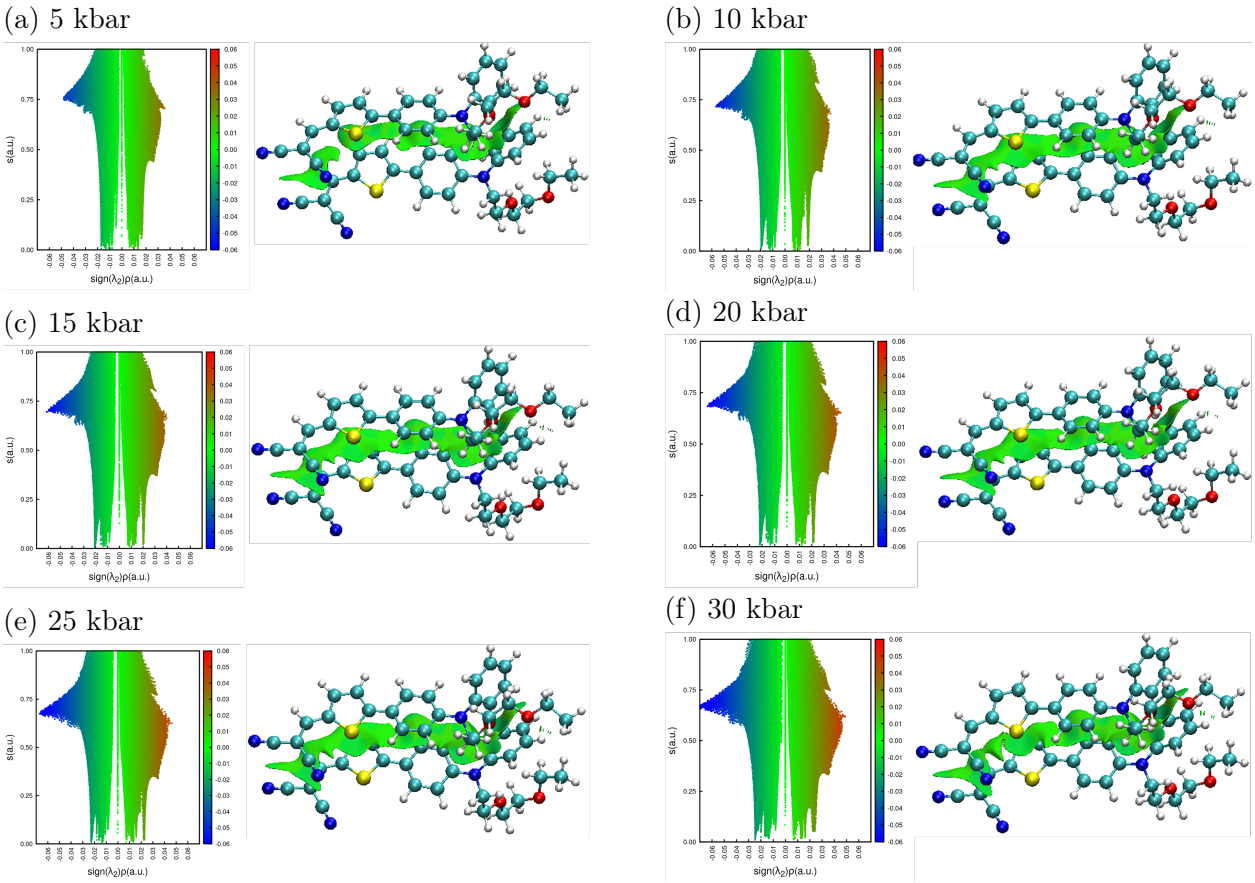

Figure S5: RDG and three-dimensional view of the interaction regions between the molecules within the dimer under increasing pressure.

3 Linear Optical Properties of the Crystalline Dimer

Table S12: Evolution with pressure (kbar) of the vertical transition energies and oscillator strengths towards the four first excited singlets.

	S_1		S_2		S_3		S_4	
Pressure	ΔE (eV)	f	ΔE (eV)	f	ΔE (eV)	f	ΔE (eV)	f
0	2.712	0.043	2.998	1.414	3.058	0.797	3.420	0.020
1	2.711	0.035	2.996	1.247	3.048	0.975	3.426	0.017
2	2.700	0.035	2.995	1.247	3.055	0.969	3.393	0.024
3	2.695	0.036	2.992	1.163	3.057	1.045	3.380	0.028
4	2.690	0.038	2.989	1.095	3.057	1.108	3.368	0.031
5	2.683	0.034	2.989	1.131	3.060	1.061	3.338	0.040
6	2.681	0.037	2.989	1.116	3.063	1.064	3.327	0.045
7	2.681	0.042	2.991	1.095	3.068	1.073	3.317	0.052
8	2.678	0.040	2.990	1.115	3.068	1.046	3.300	0.060
9	2.674	0.040	2.989	1.066	3.068	1.095	3.296	0.061
10	2.705	0.091	3.065	1.748	3.163	0.238	3.173	0.127
11	2.703	0.087	3.062	1.726	3.157	0.262	3.171	0.132
12	2.706	0.080	3.065	1.737	3.151	0.338	3.173	0.051
13	2.704	0.082	3.065	1.726	3.147	0.325	3.172	0.068
14	2.702	0.088	3.065	1.636	3.142	0.419	3.170	0.061
15	2.699	0.092	3.059	1.619	3.152	0.232	3.170	0.261
16	2.702	0.087	3.064	1.620	3.144	0.398	3.173	0.100
17	2.699	0.086	3.056	1.583	3.150	0.219	3.171	0.315
18	2.697	0.084	3.057	1.545	3.138	0.414	3.170	0.161
19	2.701	0.079	3.057	1.549	3.142	0.376	3.173	0.196
20	2.700	0.086	3.054	1.492	3.145	0.352	3.180	0.271
21	2.696	0.081	3.051	1.467	3.137	0.386	3.172	0.267
22	2.694	0.084	3.048	1.447	3.139	0.330	3.174	0.341
23	2.695	0.089	3.046	1.425	3.144	0.240	3.180	0.448
24	2.694	0.097	3.035	1.386	3.152	0.091	3.196	0.629
25	2.692	0.093	3.030	1.375	3.150	0.073	3.196	0.662
26	2.689	0.094	3.029	1.352	3.146	0.080	3.194	0.675
27	2.688	0.099	3.028	1.329	3.146	0.089	3.197	0.686
28	2.684	0.118	3.013	1.324	3.180	0.009	3.249	0.764
29	2.683	0.121	3.009	1.289	3.173	0.015	3.248	0.793
30	2.681	0.122	3.009	1.278	3.170	0.010	3.245	0.808

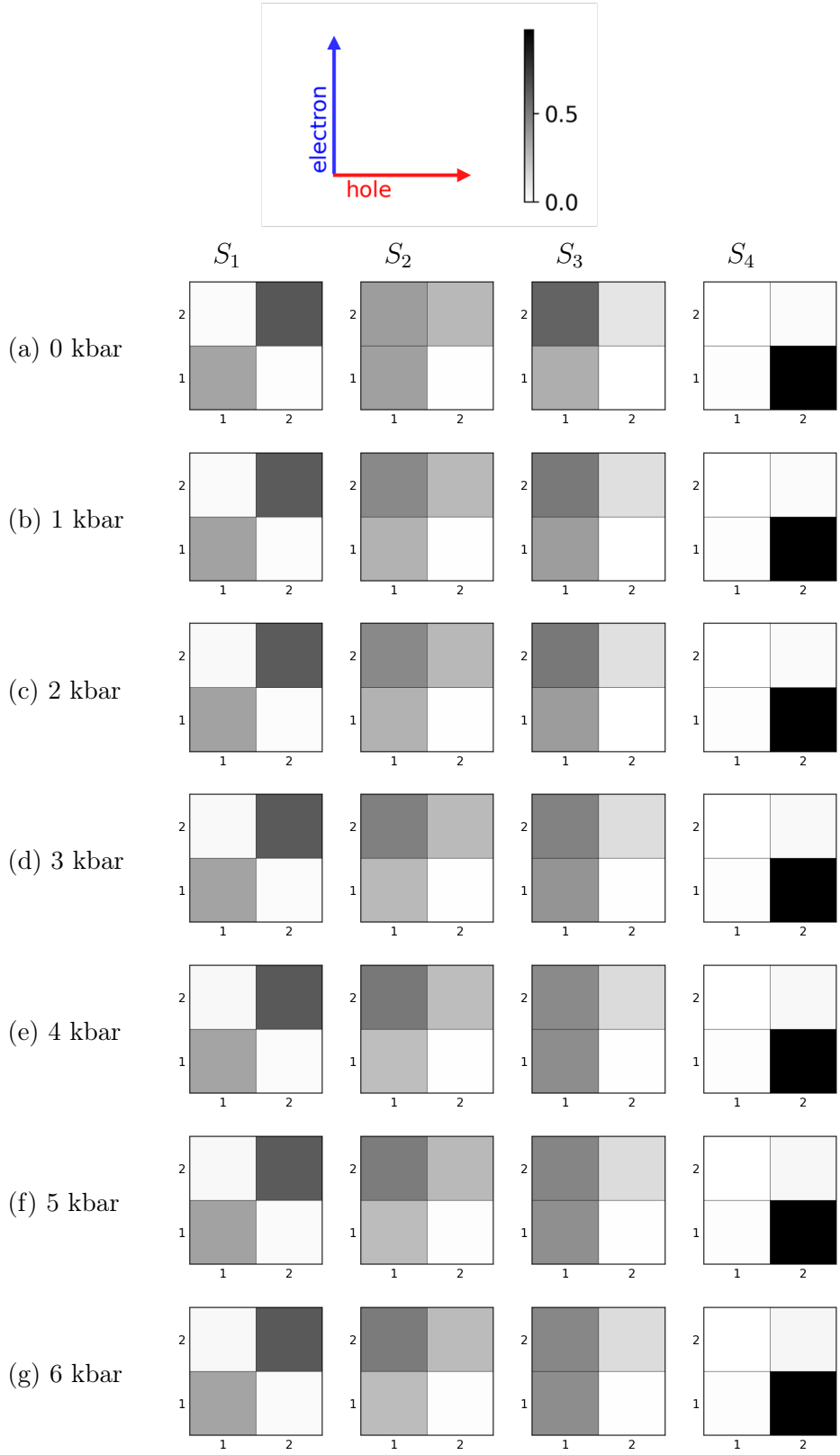

Figure S6: Electron–hole correlation plots for the S_1–S_4 excited states at different pressures ($P = 0 - 6$ kbar). Continued on next page.

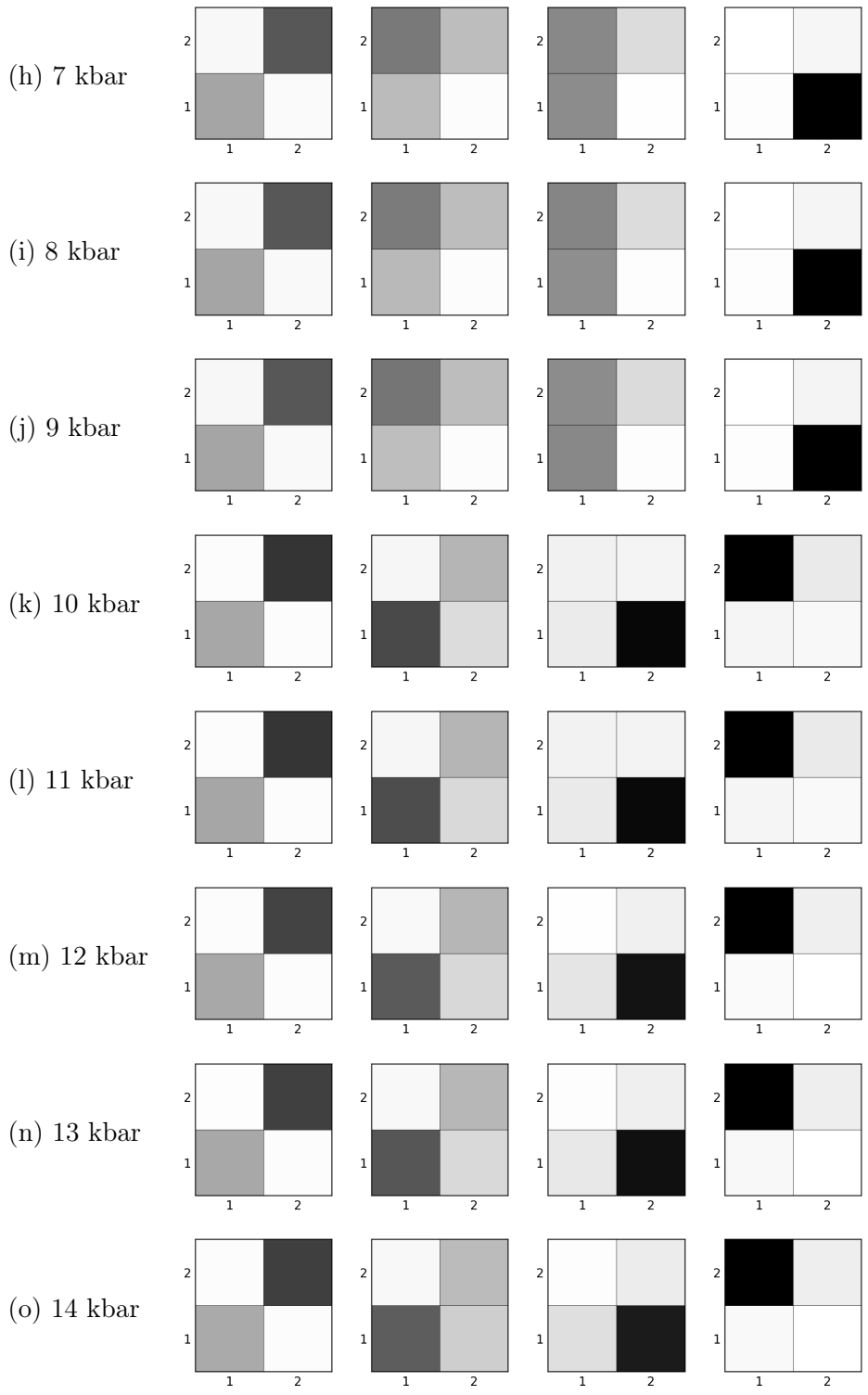

Figure S6: Electron–hole correlation plots for the S_1–S_4 excited states at different pressures ($P = 7 - 14$ kbar). Continued on next page.

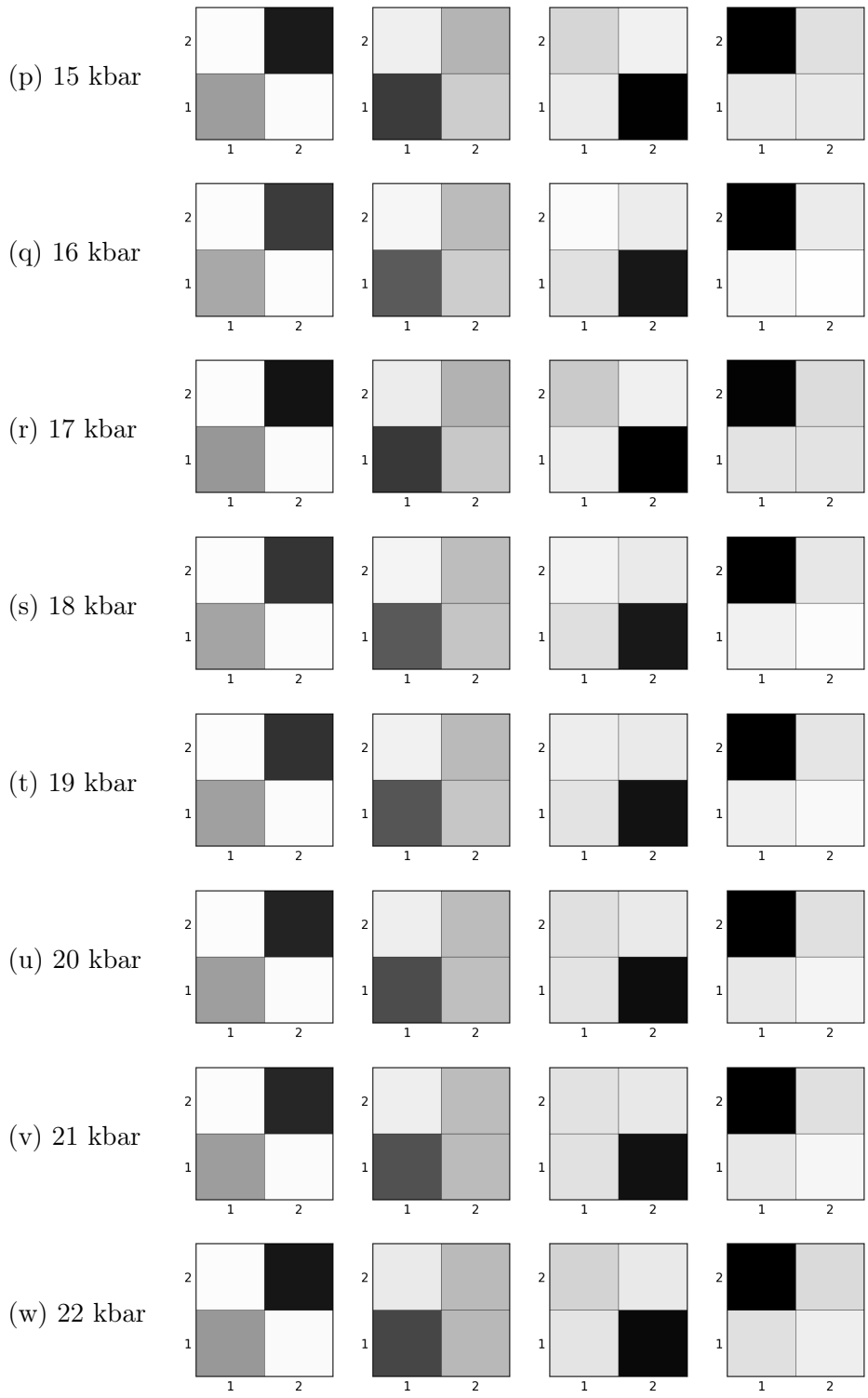

Figure S6: Electron–hole correlation plots for the S_1–S_4 excited states at different pressures ($P = 15 - 22$ kbar). Continued on next page.

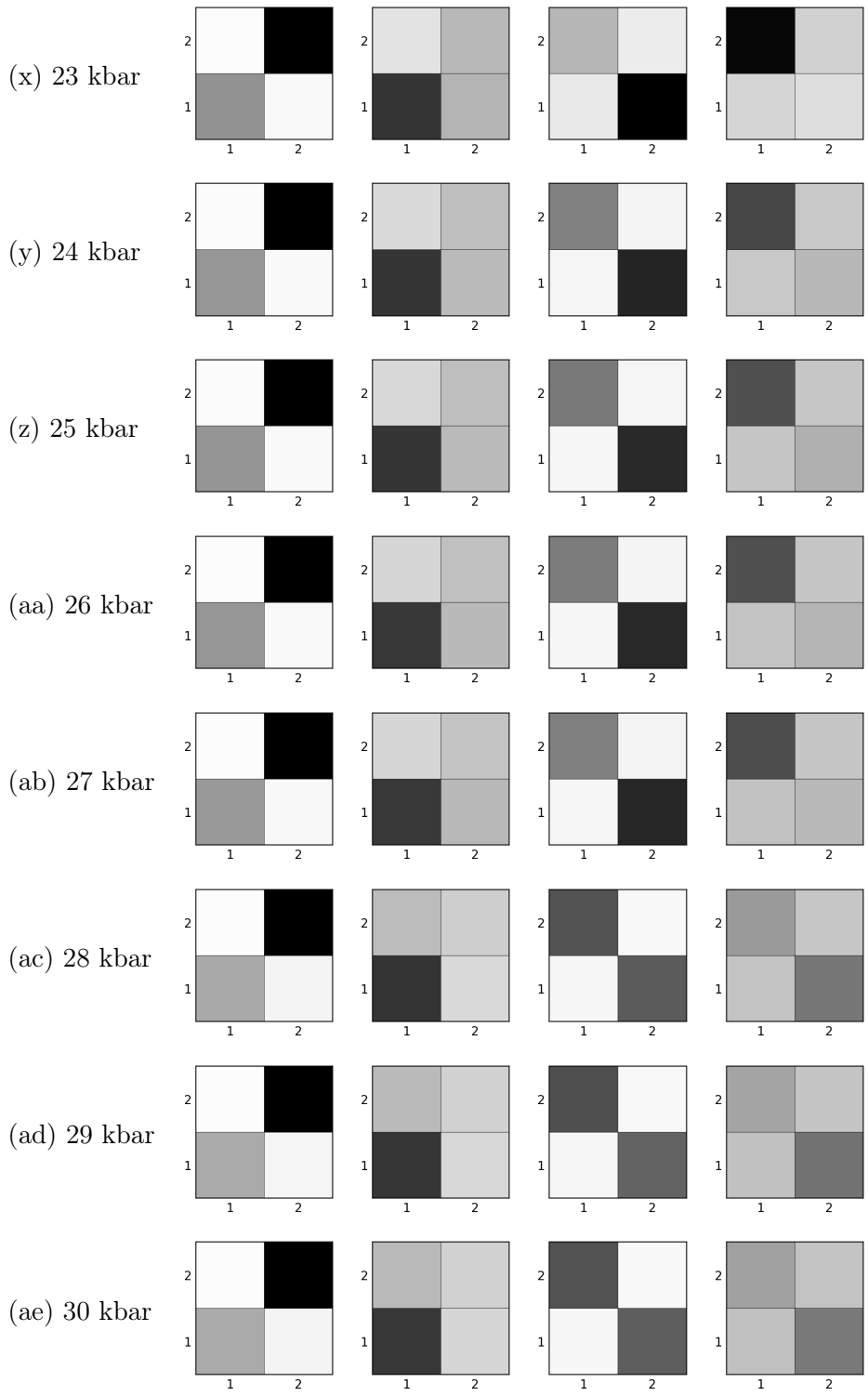

Figure S6: Electron–hole correlation plots for the S_1–S_4 excited states at different pressures ($P = 23 - 30$ kbar).

Table S13: Charge transfer contribution in the S_1-S_4 excited states.

Pressure	S_1	S_2	S_3	S_4
0	0.026	0.374	0.591	0.974
1	0.033	0.449	0.509	0.974
2	0.038	0.446	0.508	0.969
3	0.041	0.481	0.472	0.966
4	0.044	0.509	0.442	0.964
5	0.049	0.492	0.455	0.959
6	0.050	0.498	0.450	0.956
7	0.050	0.506	0.444	0.954
8	0.049	0.496	0.455	0.951
9	0.054	0.517	0.431	0.949
10	0.022	0.150	0.892	0.893
11	0.022	0.161	0.883	0.889
12	0.023	0.160	0.851	0.920
13	0.022	0.161	0.858	0.912
14	0.023	0.197	0.818	0.913
15	0.023	0.199	0.893	0.837
16	0.023	0.202	0.828	0.897
17	0.024	0.215	0.898	0.815
18	0.024	0.233	0.821	0.872
19	0.024	0.231	0.837	0.857
20	0.025	0.250	0.846	0.828
21	0.025	0.263	0.832	0.828
22	0.026	0.269	0.853	0.800
23	0.027	0.274	0.887	0.760
24	0.028	0.284	0.941	0.699
25	0.028	0.289	0.947	0.687
26	0.029	0.297	0.944	0.680
27	0.030	0.304	0.941	0.675
28	0.041	0.295	0.954	0.669
29	0.041	0.307	0.952	0.658
30	0.041	0.312	0.954	0.650

Table S14: Exciton size (Å) in the S_1-S_4 excited states.

Pressure	S_1	S_2	S_3	S_4
0	5.069	5.784	6.229	6.652
1	5.087	5.921	6.089	6.645
2	5.087	5.885	6.056	6.593
3	5.089	5.921	5.977	6.564
4	5.089	5.951	5.914	6.542
5	5.091	5.899	5.917	6.493
6	5.090	5.893	5.899	6.471
7	5.088	5.889	5.880	6.454
8	5.082	5.858	5.884	6.434
9	5.087	5.883	5.842	6.416
10	4.985	5.258	6.241	6.384
11	4.984	5.270	6.227	6.373
12	4.982	5.267	6.185	6.390
13	4.982	5.269	6.190	6.385
14	4.981	5.305	6.134	6.367
15	4.983	5.307	6.234	6.298
16	4.981	5.312	6.149	6.353
17	4.983	5.324	6.238	6.264
18	4.979	5.344	6.139	6.320
19	4.981	5.343	6.162	6.304
20	4.983	5.365	6.177	6.274
21	4.979	5.375	6.152	6.263
22	4.981	5.382	6.179	6.234
23	4.984	5.388	6.223	6.191
24	4.991	5.402	6.312	6.129
25	4.991	5.408	6.318	6.112
26	4.990	5.416	6.307	6.099
27	4.991	5.421	6.301	6.091
28	5.026	5.445	6.405	6.111
29	5.021	5.453	6.386	6.089
30	5.021	5.457	6.381	6.076

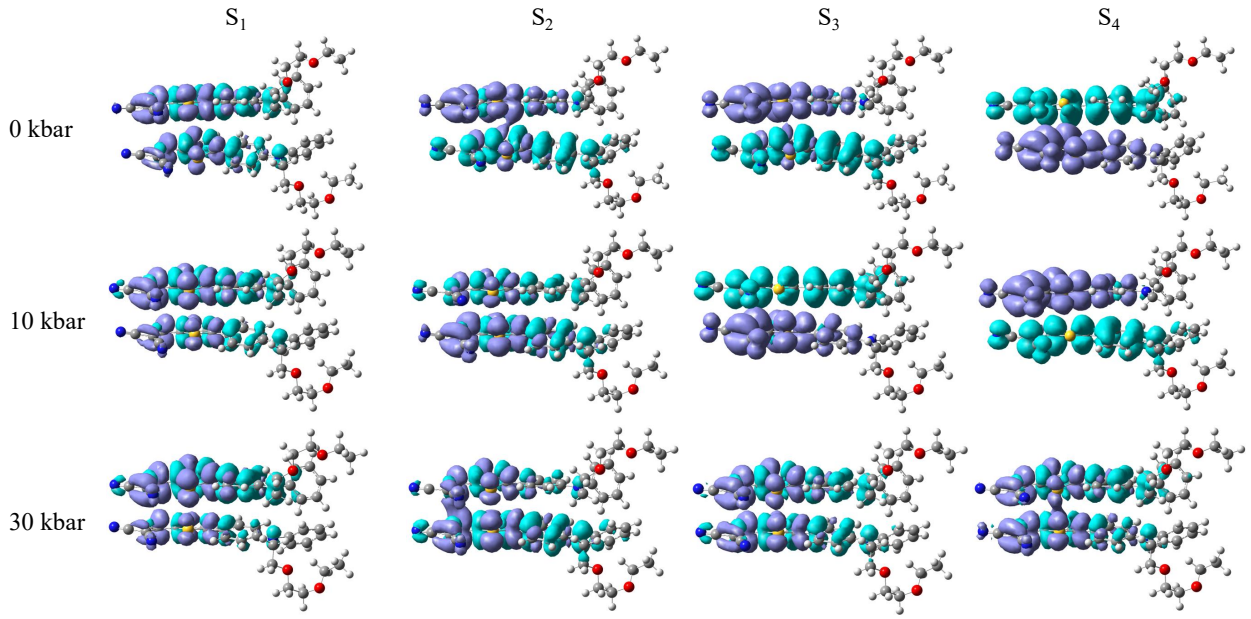

Figure S7: Electron density differences between the ground and excited states for P = 0, 10 and 30 kbar. Blue (violet) lobes are associated with negative (positive) variations, i.e. zones with decreasing (increasing) density, referred to as hole (electron), respectively. Monomer 1 is at the bottom, monomer 2 at the top.

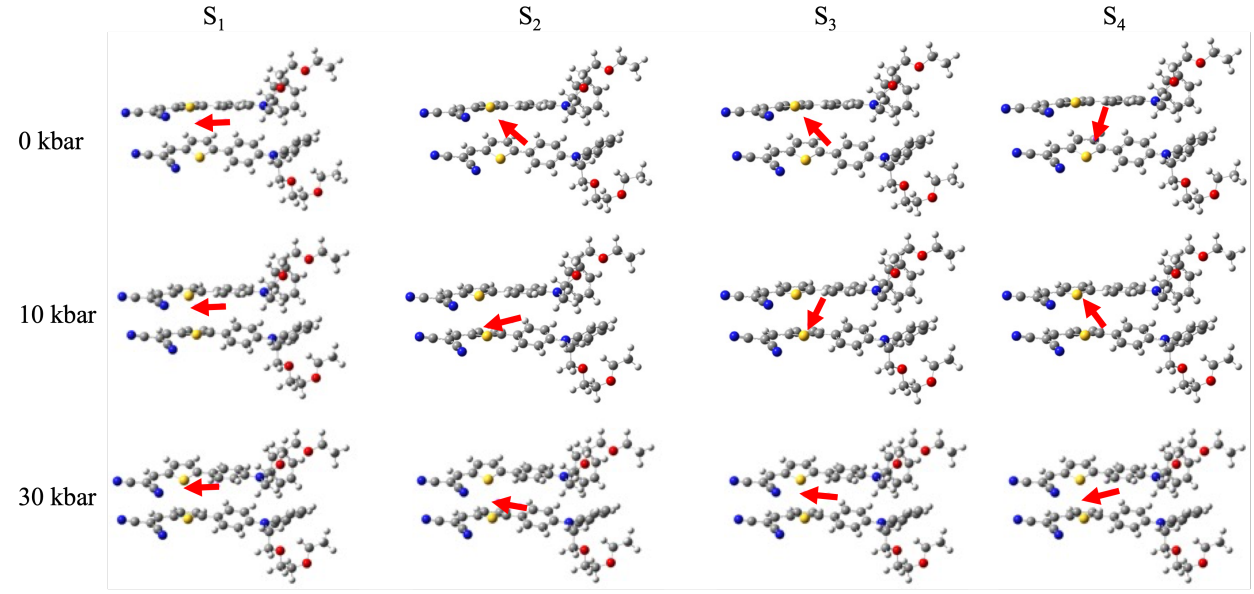

Figure S8: Charge transfer vectors connecting the barycenters of the negative and positive density distributions, oriented from the hole to the electron. Monomer 1 is at the bottom, monomer 2 at the top.

4 Nonlinear Optical Properties of the Crystalline Dimer

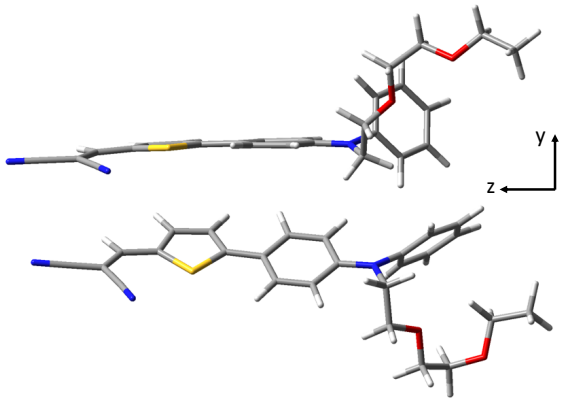

Figure S9: Cartesian frame used for the NLO calculations (see Tables below), corresponding to the Gaussian standard orientation, in which Cartesian axes are aligned along the principal moments of inertia.

Table S15: Evolution with pressure of the static components of first hyperpolarizability vector (a.u.) and of the anisotropy of the NLO response (α_β). The Cartesian frame used for the NLO calculations, corresponding to the Gaussian standard orientation, is shown in the figure above.

Pressure	$\lvert\beta_x\rvert$	$\lvert\beta_y\rvert$	$\lvert\beta_z\rvert$	β	α_β	β_{zzz}
0	686	634	24155	24173	25.9	24921
1	631	690	24187	24205	25.9	24952
2	668	663	23970	23989	25.5	24719
3	675	644	23811	23830	25.5	24551
4	670	622	23729	23747	26.0	24468
5	648	584	23583	23600	27.0	24297
6	638	569	23480	23496	27.5	24186
7	621	543	23365	23380	28.3	24068
8	616	523	23268	23283	28.8	23966
9	617	531	23243	23257	28.6	23933
10	634	337	22124	22135	30.8	22768
11	630	338	22117	22129	30.9	22761
12	619	333	22070	22081	31.4	22708
13	639	376	22064	22077	29.8	22695
14	602	355	21991	22002	31.5	22623
15	599	326	22003	22014	32.2	22660
16	589	347	21941	21952	32.1	22586
17	585	317	21935	21945	33.0	22596
18	573	337	21916	21926	33.0	22569
19	564	322	21879	21888	33.7	22536
20	551	299	21854	21863	34.8	22522
21	547	307	21828	21837	34.8	22495
22	536	289	21815	21823	35.8	22490
23	528	262	21781	21789	37.0	22466
24	515	185	21759	21765	39.8	22470
25	519	168	21731	21738	39.9	22447
26	521	179	21716	21723	39.4	22431
27	514	175	21662	21668	39.9	22380
28	519	22	21655	21662	41.7	22404
29	506	27	21621	21627	42.6	22369
30	493	36	21590	21596	43.6	22342

Table S16: Evolution with pressure of the dynamic components of first hyperpolarizability vector (a.u.) and of the anisotropy of the NLO response (α_β).

Pressure	$\lvert\beta_x\rvert$	$\lvert\beta_y\rvert$	$\lvert\beta_z\rvert$	β	α_β	β_{zzz}
0	77296	54463	857597	862794	9.1	861194
1	70908	48234	814274	818777	9.5	816058
2	77112	55680	865502	870712	9.1	868988
3	81221	60267	907884	913499	9.0	912437
4	81707	61238	914569	920252	9.0	919708
5	83553	63997	935797	941697	8.9	942476
6	88685	70065	993982	1000387	8.8	1002440
7	98395	81015	1105485	1112808	8.7	1116920
8	97115	81012	1094259	1101543	8.7	1106760
9	97874	81277	1106212	1113504	8.7	1118750
10	94026	2768	1092326	1096369	11.6	1091440
11	80792	2388	947493	950934	11.7	948111
12	86761	3990	1031329	1034980	11.9	1036740
13	83527	4935	996511	1000017	11.9	1002260
14	68857	17108	851453	854404	12.0	862218
15	62023	9321	742391	745035	11.8	741295
16	67528	13464	833074	835915	12.1	839704
17	52921	11634	641051	643336	11.8	639718
18	42242	20968	536716	538784	11.4	543720
19	45578	16989	570882	572951	11.7	574843
20	41147	14386	508528	510392	11.7	509460
21	27712	21023	356557	358250	10.3	361019
22	26453	18390	335190	336734	10.4	336981
23	29210	13501	356791	358240	11.1	354167
24	27749	6013	315003	316280	11.1	306528
25	24343	6279	273584	274736	10.9	265192
26	21830	7174	245857	246928	10.7	238003
27	20771	6087	232085	233092	10.7	224159
28	24007	5258	263529	264672	10.7	252490
29	21204	7495	230936	232029	10.3	220449
30	20316	7499	220519	221580	10.2	209907

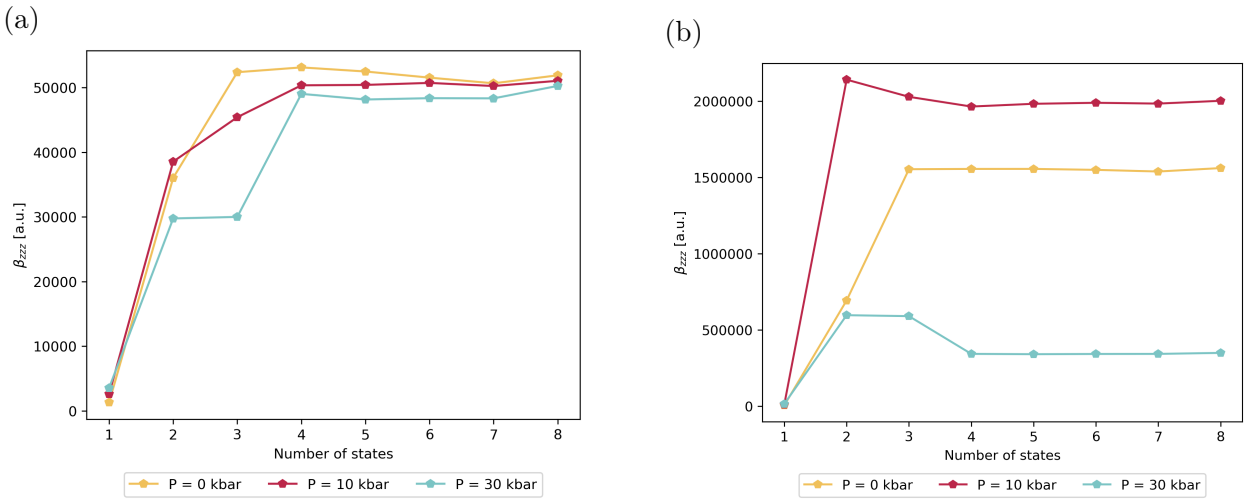

Figure S10: Evolution of the value of the static (a) and dynamic (b) β_{zzz} component as a function of the number of states included in the sum over states, at key pressures (P = 0, 10 and 30 kbar).

5 Impact of environment on the NLO properties of the Crystalline Dimer

5.1 Impact of the crystalline environment

To assess environmental effects on the NLO responses of the crystalline dimer, additional calculations were carried out using the hybrid QM/MM "Own N-layered Integrated Molecular Orbitals and Molecular Mechanics" (ONIOM) approach.[S1] The QM region comprised the DPA-Th-DCV dimer, while the surrounding molecular units directly adjacent to the central dimer were treated classically in the MM region using the Universal Force Field (UFF), as illustrated in Figure S11. As in previous studies,[S2,S3] electrostatic embedding was included in the ONIOM scheme by incorporating the partial charges of the MM region into the QM Hamiltonian, to enable accurate description of the electrostatic interactions between the QM and MM subsystems.

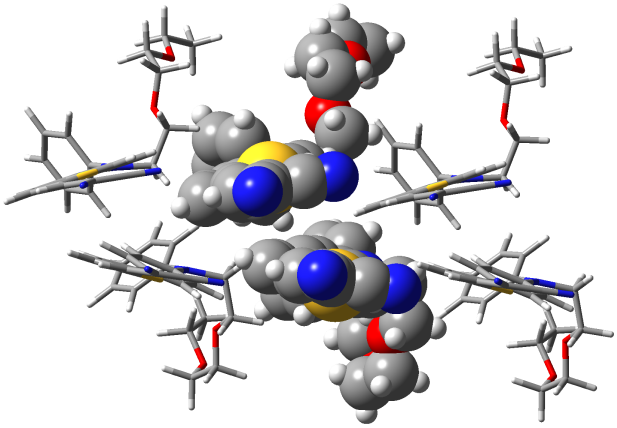

Figure S11: Supramolecular structure used in the ONIOM calculations. The central dimer, shown in van der Waals representation, defines the QM region, while the four neighboring molecular units, shown in tube representation, constitute the MM region.

As shown in Table S17, environmental effects lead to a 11% reduction of the static first hyperpolarizability at both P = 0 and P = 30 kbar. This behavior is consistent with classical electrostatics: in a parallel stacking arrangement, the dipole induced in one molecular unit generates a counteracting local field that diminishes the effective field experienced by the neighboring unit, resulting in a reduced β response (see e.g. Ref. S4). In contrast, the dynamic first hyperpolarizability increases by 9% and 15% at P = 0 and P = 30 kbar, respectively. This enhancement originates from energetic shifts of the low-lying excited states due to environment effects, which strengthen frequency-resonance effects. However, the pressure-induced variations of the NLO properties, shown in parentheses in Table S17, are very similar whether they are calculated for the isolated or for the environed DPA-Th-DCV dimer.

Table S17: Static and dynamic first hyperpolarizability (β, a.u.) of the isolated and environed DPA-Th-DCV dimer, calculated at the CAM-B3LYP-D3/6-311G(d) and ONIOM (CAM-B3LYP-D3/6-311G(d):UFF = qeq] = embedcharge) levels, using crystal geometries optimized at $P = 0$ and $P = 30$ kbar. Variations in the β values with pressure are reported in parentheses.

	Static		Dynamic	
Pressure	Dimer	Dimer + Cryst. Env.	Dimer	Dimer + Cryst. Env.
0	24173	21405	862794	939282
30	21596 (-10.7%)	19199 (-10.3%)	221580 (-74.3%)	255595 (-72.8%)

5.2 Impact of the acetonitrile molecules

Table S18: Static and dynamic first hyperpolarizability (β, a.u.) of the DPA-Th-DCV dimer isolated and surrounded by two acetonitrile (ACN) molecules, calculated at the CAM-B3LYP-D3/6-311G(d) level using crystal geometries optimized at $P = 0$ and $P = 30$ kbar. Variations in the β values with pressure are reported in parentheses.

	Static		Dynamic	
Pressure	Dimer	Dimer + 2ACN	Dimer	Dimer + 2ACN
0	24173	25618	862794	839595
30	21596 (-10.7%)	23035 (-10.1%)	221580 (-74.3%)	217095 (-74.1%)

6 More Details on the SOS Formalism

The general expression of the diagonal first hyperpolarizability component β_{zzz} in the case of the SHG process reads:

$$\beta_{zzz}^{SOS}(-2\omega;\omega,\omega) = 2\sum_{n\neq 0}\sum_{m\neq 0}\left\{\frac{\mu_{0n}^{z}(\mu_{nm}^{z}-\mu_{00}^{z}\delta_{nm})\mu_{m0}^{z}}{(\Delta E_{0n}-2\hbar\omega)(\Delta E_{0m}-\hbar\omega)}\right.$$
$$\left.+\frac{\mu_{0n}^{z}(\mu_{nm}^{z}-\mu_{00}^{z}\delta_{nm})\mu_{m0}^{z}}{(\Delta E_{0n}+\hbar\omega)(\Delta E_{0m}-\hbar\omega)}+\frac{\mu_{0n}^{z}(\mu_{nm}^{z}-\mu_{00}^{z}\delta_{nm})\mu_{m0}^{z}}{(\Delta E_{0n}+\hbar\omega)(\Delta E_{0m}+2\hbar\omega)}\right\} \quad (1)$$

or equivalently

$$\beta_{zzz}^{SOS}(-2\omega;\omega,\omega) = \sum_{n\neq 0}\beta^{(n)}(-2\omega;\omega,\omega) \tag{2}$$

with

$$\beta^{(n)}(-2\omega;\omega,\omega) = 2\sum_{m\neq 0}\Bigg\{\frac{\mu_{0n}^{z}(\mu_{nm}^{z}-\mu_{00}^{z}\delta_{nm})\mu_{m0}^{z}}{(\Delta E_{0n}-2\hbar\omega)(\Delta E_{0m}-\hbar\omega)} + \frac{\mu_{0n}^{z}(\mu_{nm}^{z}-\mu_{00}^{z}\delta_{nm})\mu_{m0}^{z}}{(\Delta E_{0n}+\hbar\omega)(\Delta E_{0m}-\hbar\omega)} + \frac{\mu_{0n}^{z}(\mu_{nm}^{z}-\mu_{00}^{z}\delta_{nm})\mu_{m0}^{z}}{(\Delta E_{0n}+\hbar\omega)(\Delta E_{0m}+2\hbar\omega)}\Bigg\} \tag{3}$$

Considering the cases $n = m$ and $n \neq m$, the above expression can be separated into two contributions:

$$\beta^{(n)}(-2\omega;\omega,\omega) = 6\frac{\mu_{0n}^{z}\Delta\mu_{0n}^{z}\mu_{0n}^{z}}{\Delta E_{0n}\Delta E_{0n}}F^{(n)}(\omega) + 6\sum_{m\neq 0;\, m\neq n}\frac{\mu_{0n}^{z}\mu_{nm}^{z}\mu_{0m}^{z}}{\Delta E_{0n}\Delta E_{0m}}F^{(n,m)}(\omega) \tag{4}$$

where $\Delta\mu_{0n}^{z} = \mu_{n}^{z} - \mu_{0}^{z}$ is the variation of the dipole moment along the z-axis upon the $S_0 \rightarrow S_n$ optical transition. $F^{(n)}(\omega)$ and $F^{(n,m)}$ are frequency dispersion factors, which depend on the energy of the incident laser field, $\hbar\omega$:

$$F^{(n)}(\omega) = \frac{\Delta E_{0n}^{4}}{(\Delta E_{0n}^{2}-(\hbar\omega)^{2})(\Delta E_{0n}^{2}-(2\hbar\omega)^{2}} \tag{5}$$

$$F^{(n,m)} = \frac{\Delta E_{0n}\Delta E_{0m}(\Delta E_{0n}\Delta E_{0m}+\hbar\omega\Delta E_{0n}-\hbar\omega\Delta E_{0m})}{(\Delta E_{0n}+\hbar\omega)(\Delta E_{0m}-\hbar\omega)(\Delta E_{0n}-2\hbar\omega)(\Delta E_{0m}+2\hbar\omega)} \tag{6}$$

These terms describe resonance effects at both the fundamental and harmonic light. They are equal to 1 in the static limit ($\omega = 0$). Finally, the contribution of an individual state S_k is obtained by the difference in the total SOS hyperpolarizabilities including k and $k-1$ states:

$$\beta_{zzz}^{(k)}(-2\omega;\omega,\omega) = \sum_{n\neq 0}^{k}\beta^{(n)}(-2\omega;\omega,\omega) - \sum_{n\neq 0}^{k-1}\beta^{(n)}(-2\omega;\omega,\omega) \tag{7}$$

References

(S1) Chung, L. W.; Sameera, W. M. C.; Ramozzi, R.; Page, A. J.; Hatanaka, M.; Petrova, G. P.; Harris, T. V.; Li, X.; Ke, Z.; Liu, F.; Li, H.-B.; Ding, L.; Morokuma, K. The ONIOM Method and Its Applications. *Chem. Rev.* **2015**, *115*, 5678–5796.

(S2) Aziz, A.; Sidat, A.; Talati, P.; Crespo-Otero, R. Understanding the solid state luminescence and piezochromic properties in polymorphs of an anthracene derivative. *Phys. Chem. Chem. Phys.* **2022**, *24*, 2832–2842.

(S3) Owona, J.; Casanova, D.; Truflandier, L.; Castet, F.; Tonnelé, C. Modelling of pressure-induced charge transfer character in piezoluminescent pyridylvinylanthracene crystals. *J. Mater. Chem. C* **2024**, *12*, 13495–13507.

(S4) Castet, F.; Champagne, B. Simple Scheme To Evaluate Crystal Nonlinear Susceptibilities: Semiempirical AM1 Model Investigation of 3-Methyl-4-nitroaniline Crystal. *J. Phys. Chem. A* **2001**, *105*, 1366–1370.